

# Modified midpoint integration rule for the trilinear element in large deformation elasticity

Mirza Cenanovic, Peter Hansbo, David Samvin

*Department of Mechanical Engineering, Jönköping University, SE-55111  
Jönköping, Sweden*

---

## Abstract

In this paper we suggest two modified one-point Gauss integration rules for the  $Q_1$  bi- or trilinear element. The modifications both stabilize the hourglass modes of the one-point rule, and one of them is accurate also on severely distorted elements. We investigate the performance of the integration rules for the hexahedron element, and combine standard one-point integration of the volumetric terms with the modified rules for the isochoric terms to handle near incompressible situations.

*Key words:* finite element method, hexahedral element, elasticity, numerical integration

---

## 1 Introduction

We consider the construction of an hourglass control method in the form of a modified Gaussian rule including derivative information to allow for one point integration of the full element matrices without loss of stability. The one point rule suffers from loss of stability leading to so-called hourglass modes. In order to remedy this, hourglass control methods have been proposed. In the context of large deformations, these are typically based on introducing auxiliary strain fields, cf. [1,2,3], or to use Taylor expansions of the strain field, for linear problems by Schultz [4] and by Liu, Ong, and Uras [5], with extension to large deformation problems in Liu, Belytschko, Ong, and Law [6] and Reese, Wriggers, and Reddy [7]. In contrast, we employ a modification of the one point Gauss rule using derivative information with selective differentiation, an idea introduced and analyzed by Hansbo [8] for a linear Poisson problem, and subsequently used in combination with a non-conforming affine tetrahedron element for a large deformation model in Hansbo and

Larsson [9]. For non-affine elements, there is however a strong stiffening effect on slender structures when the element geometry is distorted, as shown in the numerical examples below (cf. also Reese et al. [7]). The purpose of this paper is to modify the scheme in [9] so that the sensitivity to element geometry is remedied.

An outline of the paper is as follows. In Section 2 we consider the linear elasticity problem to introduce the basic ideas of our integration scheme; in Section 3 we introduce our large deformation problem, which is formulated in terms of the first Piola–Kirchhoff stress corresponding to an isotropic Mooney–Rivlin model, and show how the numerical integration scheme is implemented in this case. In Section 4 we present numerical examples and in Section 5 we give some concluding remarks. Implementation details are provided in an Appendix.

## 2 The small deformation elasticity problem

### 2.1 Continuous model

We consider a elasticity problem on a domain  $\Omega \subset \mathbb{R}^n$ . For notational simplicity we shall set  $n = 3$ , but the two-dimensional case will also be considered in the numerical examples. We first consider the following linearized elasticity problem: Find the displacement  $\mathbf{u}$  such that

$$\boldsymbol{\sigma} = \lambda \nabla \cdot \mathbf{u} \mathbf{I} + 2\mu \boldsymbol{\varepsilon}(\mathbf{u}) \quad \text{in } \Omega, \quad (1)$$

$$-\nabla \cdot \boldsymbol{\sigma} = \mathbf{f} \quad \text{in } \Omega \quad (2)$$

$$\mathbf{u} = \mathbf{0} \quad \text{on } \partial\Omega_D \quad (3)$$

$$\boldsymbol{\sigma} \cdot \mathbf{n} = \mathbf{g} \quad \text{on } \partial\Omega_N \quad (4)$$

$$(5)$$

Here  $\lambda$  and  $\mu$  are the Lamé parameters, which we assume constant in  $\Omega$ . In terms of the modulus of elasticity,  $E$ , and Poisson's ratio,  $\nu$ , we have

$$\lambda = \frac{E\nu}{(1-2\nu)(1+\nu)}, \quad \mu = \frac{E}{2(1+\nu)}.$$

Furthermore,  $\boldsymbol{\varepsilon}(\mathbf{u}) = [\varepsilon^{ij}(\mathbf{u})]_{i,j=1}^3$  is the strain tensor with components

$$\varepsilon_{ij}(\mathbf{u}) = \frac{1}{2} \left( \frac{\partial u_i}{\partial x_j} + \frac{\partial u_j}{\partial x_i} \right),$$

$\nabla \cdot \boldsymbol{\sigma} = [\sum_{j=1}^3 \partial \sigma_{ij} / \partial x_j]_{i=1}^3$ ,  $\mathbf{I} = [\delta_{ij}]_{i,j=1}^3$  with  $\delta_{ij} = 1$  if  $i = j$  and  $\delta_{ij} = 0$  if  $i \neq j$ , and  $\mathbf{n}$  is the outward normal to  $\Omega$  on the boundary  $\partial\Omega = \partial\Omega_D \cup \partial\Omega_N$

On weak form the problem is to find  $\mathbf{u} \in V$ ,

$$V = \{\mathbf{v} \in [H^1(\Omega)]^3 : \mathbf{v} = \mathbf{0} \text{ on } \partial\Omega_D\},$$

such that

$$a(\mathbf{u}, \mathbf{v}) = l(\mathbf{v}) \quad \forall \mathbf{v} \in V, \quad (6)$$

where

$$a(\mathbf{v}, \mathbf{w}) = 2\mu \int_{\Omega} \boldsymbol{\varepsilon}(\mathbf{v}) : \boldsymbol{\varepsilon}(\mathbf{w}) \, d\Omega + \lambda \int_{\Omega} \nabla \cdot \mathbf{v} \, \nabla \cdot \mathbf{w} \, d\Omega \quad (7)$$

and

$$l(\mathbf{v}) = \int_{\Omega} \mathbf{f} \cdot \mathbf{v} \, d\Omega + \int_{\partial\Omega_N} \mathbf{g} \cdot \mathbf{v} \, ds. \quad (8)$$

## 2.2 Finite element model

Let  $\mathcal{T}_h$  be a conforming mesh on  $\Omega \subset \mathbb{R}^n$ . On a reference brick  $\hat{T}$  we have 8 basis functions  $\hat{\varphi}_i(\boldsymbol{\xi})$ , and we define a map  $\mathbf{F}_T : (\xi, \eta, \zeta) \rightarrow (x, y, z)$  from the reference configuration to a physical element  $T$  by

$$\mathbf{x} = \mathbf{F}_T(\boldsymbol{\xi}) := \sum_{i=1}^8 \hat{\varphi}_i(\boldsymbol{\xi}) \mathbf{x}_i,$$

where  $\mathbf{x}_i$  is the physical location of element node  $i$ . Under this map, we define  $\varphi_i(\mathbf{x}) = \hat{\varphi}_i(\boldsymbol{\xi})$ . Denoting  $Q_1$  as the set of trilinear functions, our discrete space can then be written

$$V_h := \{\mathbf{v} \in V : \mathbf{v}|_T \in [Q_1(\mathbf{F}_T^{-1}T)]^3, \forall T \in \mathcal{T}_h\}, \quad (9)$$

where  $\mathbf{F}_T^{-1}T$  denotes the map back to the reference element  $\hat{T}$ , and we can introduce the finite element method as: find  $\mathbf{u}^h \in V^h$  such that

$$a(\mathbf{u}^h, \mathbf{v}) = l(\mathbf{v}), \quad \forall \mathbf{v} \in V^h. \quad (10)$$

In the practical implementation we let

$$\mathbf{u}^h = \begin{bmatrix} \varphi_1 & 0 & 0 & \varphi_2 & 0 & 0 & \dots \\ 0 & \varphi_1 & 0 & 0 & \varphi_2 & 0 & \dots \\ 0 & 0 & \varphi_1 & 0 & 0 & \varphi_2 & \dots \end{bmatrix} \begin{bmatrix} U_{x_1,1} \\ U_{x_2,1} \\ U_{x_3,1} \\ U_{x_1,2} \\ U_{x_2,2} \\ U_{x_3,2} \\ \vdots \end{bmatrix} = \mathbf{\Phi} \mathbf{a}$$

where  $(U_{x_1,i}, U_{x_2,i}, U_{x_3,i})$  is the approximate displacement in node number  $i$ . We then arrive at the discrete matrix problem  $\mathbf{K} \mathbf{a} = \mathbf{b}$  where  $\mathbf{b}$  contains the load contributions and

$$\mathbf{K} = \int_{\Omega} \mathbf{B}^T \mathbf{D} \mathbf{B} \, dx_1 dx_2 dx_3 \quad (11)$$

where, with  $\tilde{\nabla}$  the matrix differential operator

$$\tilde{\nabla} := \begin{bmatrix} \frac{\partial}{\partial x_1} & 0 & 0 & \frac{\partial}{\partial x_2} & 0 & \frac{\partial}{\partial x_3} \\ 0 & \frac{\partial}{\partial x_2} & 0 & \frac{\partial}{\partial x_1} & \frac{\partial}{\partial x_3} & 0 \\ 0 & 0 & \frac{\partial}{\partial x_3} & 0 & \frac{\partial}{\partial x_1} & \frac{\partial}{\partial x_1} \end{bmatrix}$$

$\mathbf{B} = \tilde{\nabla}^T \mathbf{\Phi}$  and  $\mathbf{D}$  is a matrix of the elastic moduli (cf. [10]). The entries of  $\mathbf{B}$  are typically computed using the inverse of the Jacobian mapping from a reference element, which we shall assume is given on the domain  $0 \leq \xi_i \leq 1$ . We define

$$\mathbf{J} := \begin{bmatrix} \frac{\partial x_1}{\partial \xi_1} & \frac{\partial x_2}{\partial \xi_1} & \frac{\partial x_3}{\partial \xi_1} \\ \frac{\partial x_1}{\partial \xi_2} & \frac{\partial x_2}{\partial \xi_2} & \frac{\partial x_3}{\partial \xi_2} \\ \frac{\partial x_1}{\partial \xi_3} & \frac{\partial x_2}{\partial \xi_3} & \frac{\partial x_3}{\partial \xi_3} \end{bmatrix}$$

and then

$$\begin{bmatrix} \frac{\partial \varphi_i}{\partial x_1} \\ \frac{\partial \varphi_i}{\partial x_2} \\ \frac{\partial \varphi_i}{\partial x_3} \end{bmatrix} = \mathbf{J}^{-1} \begin{bmatrix} \frac{\partial \hat{\varphi}_i}{\partial \xi_1} \\ \frac{\partial \hat{\varphi}_i}{\partial \xi_2} \\ \frac{\partial \hat{\varphi}_i}{\partial \xi_3} \end{bmatrix} =: \mathbf{J}^{-1} \nabla_{\xi} \hat{\varphi}$$

and  $\mathbf{K}$  is assembled from element contributions

$$\mathbf{K}_T := \int_T \mathbf{B}^T \mathbf{D} \mathbf{B} \, dx_1 dx_2 dx_3 = \int_{\hat{T}} \mathbf{B}^T \mathbf{D} \mathbf{B} \, J \, d\xi_1 d\xi_2 d\xi_3, \quad (12)$$

where  $J := \det \mathbf{J}$ .

### 2.3 Numerical integration

The one point Gaussian (midpoint) rule for the element-wise evaluation of (11) is well known to result in a singular matrix, with singularity related to the *hourglass mode*. This is unfortunate since the midpoint rule would be sufficiently accurate in terms of convergence of the method, and could be used were it not for the stability problem. For this reason, the use of  $2 \times 2 \times 2$  Gauss points is usually recommended. However, one may alternatively use the following integration rule

$$\begin{aligned} \int_a^b f(\xi) \, d\xi &\approx \int_a^b \left( f(\xi_m) + f'(\xi_m)(\xi - \xi_m) + \frac{1}{2} f''(\xi_m)(\xi - \xi_m)^2 \right) d\xi \\ &= h f(\xi_m) + \frac{h^3}{24} f''(\xi_m), \end{aligned}$$

which is exact for polynomials up to second degree. On our reference element we can use the Taylor series expansion of  $f(\boldsymbol{\xi})$  around  $\boldsymbol{\xi}_m$ ,

$$\begin{aligned} f(\boldsymbol{\xi}) &\approx f(\boldsymbol{\xi}_m) + (\boldsymbol{\xi} - \boldsymbol{\xi}_m) \cdot \nabla_{\xi} f(\boldsymbol{\xi}_m) \\ &\quad + \frac{1}{2} (\boldsymbol{\xi} - \boldsymbol{\xi}_m) \cdot ((\boldsymbol{\xi} - \boldsymbol{\xi}_m) \cdot \nabla_{\xi} (\nabla_{\xi} f(\boldsymbol{\xi}_m))). \end{aligned} \quad (13)$$

Now, the second term in the expansion integrates to zero on the reference element by definition of the center of gravity, as do the mixed derivative terms in the third term. We are left with

$$\int_0^1 \int_0^1 \int_0^1 f(\boldsymbol{\xi}) \, d\xi_1 d\xi_2 d\xi_3 \approx f(\boldsymbol{\xi}_m) + \frac{1}{24} \sum_{i=1}^3 \frac{\partial^2 f}{\partial \xi_i^2}(\boldsymbol{\xi}_m).$$

We now want to apply this rule to the element-wise integration of contributions to  $\mathbf{K}$ . We have

$$\begin{aligned} \frac{\partial^2}{\partial \xi_i^2} (\mathbf{B}^T \mathbf{D} \mathbf{B} J) &= \left( 2 \left( \frac{\partial \mathbf{B}}{\partial \xi_i} \right)^T \mathbf{D} \frac{\partial \mathbf{B}}{\partial \xi_i} + \left( \frac{\partial^2 \mathbf{B}}{\partial \xi_i^2} \right)^T \mathbf{D} \mathbf{B} + \mathbf{B}^T \mathbf{D} \frac{\partial^2 \mathbf{B}}{\partial \xi_i^2} \right) J \\ &\quad + 2 \left( \left( \frac{\partial \mathbf{B}}{\partial \xi_i} \right)^T \mathbf{D} \mathbf{B} + \mathbf{B}^T \mathbf{D} \frac{\partial \mathbf{B}}{\partial \xi_i} \right) \frac{\partial J}{\partial \xi_i} + \mathbf{B}^T \mathbf{D} \mathbf{B} \frac{\partial^2 J}{\partial \xi_i^2}, \end{aligned} \quad (14)$$

and we thus seek suitable simplifications of this expression, notably avoiding second derivatives of involved quantities.

Defining

$$\mathbf{A}_i := \mathbf{J}^{-1} \frac{\partial \mathbf{J}}{\partial \xi_i},$$

we have that

$$\frac{\partial \mathbf{J}^{-1}}{\partial \xi_i} = -\mathbf{A}_i \mathbf{J}^{-1},$$

and it follows that

$$\frac{\partial}{\partial \xi_i} \begin{bmatrix} \frac{\partial \varphi_i}{\partial x_1} \\ \frac{\partial \varphi_i}{\partial x_2} \\ \frac{\partial \varphi_i}{\partial x_3} \end{bmatrix} = \mathbf{J}^{-1} \begin{bmatrix} \frac{\partial^2 \hat{\varphi}_i}{\xi_1 \xi_i} \\ \frac{\partial^2 \hat{\varphi}_i}{\xi_2 \xi_i} \\ \frac{\partial^2 \hat{\varphi}_i}{\xi_3 \xi_i} \end{bmatrix} - \mathbf{A}_i \begin{bmatrix} \frac{\partial \varphi_i}{\partial x_1} \\ \frac{\partial \varphi_i}{\partial x_2} \\ \frac{\partial \varphi_i}{\partial x_3} \end{bmatrix}. \quad (15)$$

These quantities are then used to build derivatives of the  $\mathbf{B}$  matrices with respect to reference coordinates.

*In the following, it is understood that all terms in the approximate integration schemes are evaluated at the midpoint of the reference element.*

We note that in case  $\mathbf{A}_i$  is nonzero, there is an explicit dependence on  $i$  in the derivative of  $\mathbf{B}$ . In the following we shall therefore write  $\partial \mathbf{B}(\mathbf{A}_i)/\partial \xi_i$  for clarity. The simplest possible integration schemes using approximations of (14) are

A. Approximate  $\mathbf{J}$  by a constant matrix. This leads to  $\mathbf{A}_i = \mathbf{0}$  and

$$\frac{\partial^2}{\partial \xi_i^2} (\mathbf{B}^T \mathbf{D} \mathbf{B} J) \approx 2 \left( \frac{\partial \mathbf{B}(\mathbf{0})}{\partial \xi_i} \right)^T \mathbf{D} \frac{\partial \mathbf{B}(\mathbf{0})}{\partial \xi_i} J.$$

B. Approximate  $\partial \mathbf{J}^{-1}/\partial \xi_i$  by a constant matrix and  $J$  by a constant. This leads to

$$\frac{\partial^2}{\partial \xi_i^2} (\mathbf{B}^T \mathbf{D} \mathbf{B} J) \approx 2 \left( \frac{\partial \mathbf{B}(\mathbf{A}_i)}{\partial \xi_i} \right)^T \mathbf{D} \frac{\partial \mathbf{B}(\mathbf{A}_i)}{\partial \xi_i} J.$$

Our numerical experience is that including derivatives of  $J$  does not improve the accuracy, so we will limit the discussion to these two approximations.

The element matrix computed on the unit reference element  $\hat{T}$  can hence be approximated as follows

$$\begin{aligned} \mathbf{K}_T &= \int_{\hat{T}} \mathbf{B}^T \mathbf{D} \mathbf{B} J \, d\xi_1 d\xi_2 d\xi_3 \\ &\approx J \mathbf{B}^T \mathbf{D} \mathbf{B} + \frac{J}{12} \sum_{i=1}^3 \left( \frac{\partial \mathbf{B}(\mathbf{A}_i)}{\partial \xi_i} \right)^T \mathbf{D} \frac{\partial \mathbf{B}(\mathbf{A}_i)}{\partial \xi_i}. \end{aligned} \quad (16)$$

The first term in the approximation is the one obtained by a standard one point rule, and the remaining are called hourglass stabilization matrices. This integration scheme, with  $\mathbf{A}_i = \mathbf{0}$ , was suggested in [8,9], and is related to classical hourglass control methods, cf. [4,5,6]. Unfortunately, this method leads to overly stiff responses in cases of large deviation from affine mappings. The same problem exists in other approaches to hourglass control, cf. Reese, Wriggers, and Reddy [7]. As we shall see in Section 4, this is remedied by simply changing  $\partial \mathbf{B}(\mathbf{0})/\partial \xi_i$  to  $\partial \mathbf{B}(\mathbf{A}_i)/\partial \xi_i$  in (16), which comes at the cost of a small number of additional  $3 \times 3$  matrix multiplications.

### 3 A large deformation elasticity problem

#### 3.1 Continuous model

Let an elastic body in its undeformed configuration, in a Cartesian coordinate system  $\mathbf{X}$ , occupy a three-dimensional domain  $\Omega_0 \subset \mathbb{R}^3$ , with outward pointing normal  $\mathbf{N}$  to the boundary  $\partial\Omega_0$ . The corresponding position in the deformed domain is denoted by  $\mathbf{x}$ , and the displacement field  $\mathbf{u}$  is then given by  $\mathbf{u}(\mathbf{X}) = \mathbf{x}(\mathbf{X}) - \mathbf{X}$ . Let us define the Jacobian of  $\mathbf{f}$  as

$$\frac{\partial \mathbf{f}}{\partial \mathbf{X}} := \begin{bmatrix} \frac{\partial f_1}{\partial X_1} & \frac{\partial f_1}{\partial X_2} & \frac{\partial f_1}{\partial X_3} \\ \frac{\partial f_2}{\partial X_1} & \frac{\partial f_2}{\partial X_2} & \frac{\partial f_2}{\partial X_3} \\ \frac{\partial f_3}{\partial X_1} & \frac{\partial f_3}{\partial X_2} & \frac{\partial f_3}{\partial X_3} \end{bmatrix}. \quad (17)$$

The deformation gradient on  $\Omega_0$  is then given by

$$\mathbf{F}(\mathbf{u}) := \frac{\partial \mathbf{x}}{\partial \mathbf{X}} = \mathbf{I} + \frac{\partial \mathbf{u}}{\partial \mathbf{X}} \quad (18)$$

Consider next a potential energy functional given by

$$\Pi(\mathbf{u}) := \Psi(\mathbf{u}) - \Pi^{\text{ext}}(\mathbf{u}) \quad (19)$$

where  $\Psi$  is the strain energy functional and  $\Pi^{\text{ext}}$  is the potential of external loads. We will assume conservative loading so that  $\Pi^{\text{ext}}(\mathbf{u}) = l(\mathbf{u})$  is linear. We have

$$\Psi(\mathbf{u}) = \int_{\Omega_0} \hat{\Psi}_{\mathbf{X}}(\mathbf{E}(\mathbf{u})) d\Omega_0 = \int_{\Omega_0} \Psi_{\mathbf{X}}(\mathbf{C}(\mathbf{u})) d\Omega_0, \quad (20)$$

where  $\Psi_{\mathbf{X}}$  is the strain energy per unit volume. Assuming for simplicity that  $\mathbf{u}$  is zero on part of the boundary  $\partial\Omega_0$ , then minimizing the potential energy leads to the variational problem of finding  $\mathbf{u} : \Omega \rightarrow \mathbb{R}^3$  such that

$$\int_{\Omega_0} \mathbf{S}(\mathbf{u}) : \mathbf{E}'(\mathbf{u}, \mathbf{v}) d\Omega = l(\mathbf{v}), \quad (21)$$

or

$$A(\mathbf{u}, \mathbf{v}) = l(\mathbf{v}),$$

for all  $\mathbf{v} : \Omega_0 \rightarrow \mathbb{R}^3$  vanishing on  $\partial\Omega_0$ , where

$$\mathbf{S}(\mathbf{u}) := \frac{\partial \hat{\Psi}_{\mathbf{X}}}{\partial \mathbf{E}} = 2 \frac{\partial \Psi_{\mathbf{X}}}{\partial \mathbf{C}} \quad (22)$$

is the second Piola–Kirchhoff stress tensor and

$$\mathbf{E}'(\mathbf{u}, \mathbf{v}) := \frac{1}{2} \left( \mathbf{F}(\mathbf{u})^T \frac{\partial \mathbf{v}}{\partial \mathbf{X}} + \left( \frac{\partial \mathbf{v}}{\partial \mathbf{X}} \right)^T \mathbf{F}(\mathbf{u}) \right) \quad (23)$$

is the variational derivative of  $\mathbf{E}$ .

For definiteness, we use an isotropic Mooney–Rivlin model in which we choose parameters  $E$  and  $\nu$ , and define  $K = E/(3(1 - 2\nu))$ ,  $\mu = E/(2(1 + \nu))$ , and  $K_1 = K_2 = \mu/2$ . Then the Mooney–Rivlin strain energy density is given by

$$\Psi_{\mathbf{X}}(\mathbf{C}) := K_1(\hat{I}_1 - 3) + K_2(\hat{I}_2 - 3) + \frac{1}{2}K(J_C - 1)^2 \quad (24)$$

where  $J_C := \det \mathbf{C}$ ,  $\hat{I}_1 := J_C^{-1/3} I_1$ , and  $\hat{I}_2 := J_C^{-2/3} I_2$ , with  $I_1$  and  $I_2$  the first and second invariants of  $\mathbf{C}$ , cf. [10].

We can now introduce the finite element method: Find  $\mathbf{u}^h \in V^h$ , where

$$V^h = \{\mathbf{v} : \mathbf{v} \in [W_k^h]^3, \mathbf{v} \text{ is zero on } \partial\Omega_0\},$$

such that

$$A(\mathbf{u}^h, \mathbf{v}) = l_h(\mathbf{v}), \quad \forall \mathbf{v} \in V^h, \quad (25)$$



For the solution of the nonlinear problem (25) we adopt Newton iterations: we compute updates  $\Delta \mathbf{u}^h \in V^h$ , for each previous iteration  $\mathbf{u}^{h(k)}$ , such that

$$A'(\mathbf{u}^{h(k)}, \mathbf{v}, \Delta \mathbf{u}_h) = l_h(\mathbf{v}) - A(\mathbf{u}^{h(k)}, \mathbf{v}), \quad \forall \mathbf{v} \in V^h, \quad (26)$$

resulting in the iterative solutions

$$\mathbf{u}^{h(k+1)} = \mathbf{u}^{h(k)} + \Delta \mathbf{u}^h \rightarrow \mathbf{u}^h \text{ with } k.$$

In (26) we introduced the tangent form, or directional derivative, of  $A(\cdot, \cdot)$ ,

$$\begin{aligned} A'(\mathbf{u}, \mathbf{v}, \mathbf{w}) &:= \int_{\Omega_0} \mathbf{E}'(\mathbf{u}, \mathbf{v}) : \mathcal{L} : \mathbf{E}'(\mathbf{u}, \mathbf{w}) d\Omega \\ &+ \int_{\Omega_0} \mathbf{S}(\mathbf{u}) : \left( \left( \frac{\partial \mathbf{v}}{\partial \mathbf{X}} \right)^T \frac{\partial \mathbf{w}}{\partial \mathbf{X}} \right) d\Omega, \end{aligned} \quad (27)$$

where we used the material elasticity tensor defined as

$$\mathcal{L} := \frac{\partial \mathbf{S}}{\partial \mathbf{E}} = 2 \frac{\partial \mathbf{S}}{\partial \mathbf{C}}. \quad (28)$$

This linearization can be split into a volumetric part and an isochoric part which will be used for the purpose of underintegrating the volumetric part to avoid locking in near incompressibility, cf. Appendix.

Following [9] we propose to apply the integration rule to (26), after linearization. This leads to a simple perturbed Newton method which in our computational experience shows similar convergence to Newton's method applied to a fully integrated element. To define this approach, we employ Voigt notation following [10] and the element tangent stiffness matrix  $\mathbf{K}_T$  can be computed as follows:

$$\mathbf{K}_T = \int_T \left( \mathbf{B}_L^T \mathbf{L} \mathbf{B}_L + \mathbf{B}_{NL}^T \mathbf{T} \mathbf{B}_{NL} \right) dx_1 dx_2 dx_3. \quad (29)$$

Here  $\mathbf{T}$  contains three copies of the second Piola–Kirchhoff tensor  $\mathbf{S}$  on the diagonal,  $\mathbf{L}$  denotes the matrix representation of the fourth order tensor  $\mathcal{L}$ ,  $\mathbf{B}_L$  is the Voigt representation of  $\mathbf{E}'$  applied to the basis functions and  $\mathbf{B}_{NL}$  is the Voigt representation of the Jacobian of the basis functions, see [10] for details. We now apply the one point integration formula to obtain

$$\begin{aligned} \mathbf{K}_T &\approx J \left( \mathbf{B}_L^T \mathbf{L} \mathbf{B}_L + \mathbf{B}_{NL}^T \mathbf{T} \mathbf{B}_{NL} \right) \\ &+ \frac{J}{12} \sum_{i=1}^3 \left( \frac{\partial \mathbf{B}_L(\mathbf{A}_i)}{\partial \xi_i} \right)^T \mathbf{L} \frac{\partial \mathbf{B}_L(\mathbf{A}_i)}{\partial \xi_i} \\ &+ \frac{J}{12} \sum_{i=1}^3 \left( \frac{\partial \mathbf{B}_{NL}(\mathbf{A}_i)}{\partial \xi_i} \right)^T \mathbf{T} \frac{\partial \mathbf{B}_{NL}(\mathbf{A}_i)}{\partial \xi_i}. \end{aligned} \quad (30)$$

For the integration of  $a_h(\mathbf{u}^{h(k)}, \mathbf{v})$  in the right hand side of the Newton iterations, we note that taking the  $\xi_i$ -derivative of  $\mathbf{S}(\mathbf{u}) : \mathbf{E}'(\mathbf{u}, \mathbf{v})$  gives rise to the same terms as the linearization and we can approximate the contribution to the right-hand side as follows:

$$\begin{aligned} \int_T \mathbf{B}_L^T \mathbf{S} \, dx_1 dx_2 dx_3 &\approx J \mathbf{B}_L^T \mathbf{S} + \frac{J}{12} \sum_{j=1}^3 \frac{\partial \mathbf{B}_L^T(\mathbf{A}_i)}{\partial \xi_j} \mathbf{L} \frac{\partial \mathbf{B}_L(\mathbf{A}_i)}{\partial \xi_j} \mathbf{a}^k \\ &+ \frac{J}{12} \sum_{j=1}^3 \frac{\partial \mathbf{B}_{NL}^T(\mathbf{A}_i)}{\partial \xi_j} \mathbf{T} \frac{\partial \mathbf{B}_{NL}(\mathbf{A}_i)}{\partial \xi_j} \mathbf{a}^k, \end{aligned} \quad (31)$$

where  $\mathbf{a}^k$  denotes the element displacement vector at iteration  $k$  and  $\mathbf{S}$  denotes the second Piola-Kirchhoff stress tensor on Voigt form.

As is evident from (30) and (31), this approximate Newton method only requires linearized quantities that are computed in standard Newton solvers for the fully integrated element.

## 4 Numerical examples

In the numerical examples below we use “full integration” to mean an integration rule which is exact for polynomials up to and including degree 2.

### 4.1 Split into volumetric and isochoric parts

In order to avoid locking in near incompressibility, we employ underintegration of the volumetric part of  $\mathbf{L}$  and  $\mathbf{S}$  for the case of Mooney-Rivlin material and define on Voigt form

$$\begin{cases} \mathbf{S}^{\text{iso}} &= \frac{\partial}{\partial \mathbf{C}} \left( K_1(\hat{I}_1 - 3) + K_2(\hat{I}_2 - 3) \right) \\ \mathbf{S}^{\text{vol}} &= \frac{\partial}{\partial \mathbf{C}} \left( \frac{1}{2} K (J_C - 1)^2 \right) \\ \mathbf{L}^{\text{iso}} &= \frac{\partial}{\partial \mathbf{C}} \mathbf{S}^{\text{iso}} \\ \mathbf{L}^{\text{vol}} &= \frac{\partial}{\partial \mathbf{C}} \mathbf{S}^{\text{vol}}, \end{cases}$$

see Appendix for details on the implementation of the Voigt form.

## 4.2 Underintegration

We compare full integration of the volumetric and isochoric parts of the discrete second Piola-Kirchhoff stress  $\mathbf{T}$  and tangent stiffness  $\mathbf{L}$  to the full integration of the isochoric parts  $\mathbf{S}^{\text{iso}}$  and  $\mathbf{L}^{\text{iso}}$  but one point integration of the volumetric parts  $\mathbf{T}^{\text{vol}}$  and  $\mathbf{L}^{\text{vol}}$ , we denote this classical approach by “1-PVol”.

For our approach, we denote the full stabilization term as

$$s_h := \frac{J}{12} \sum_{j=1}^3 \left( \frac{\partial \mathbf{B}_L^T(\mathbf{A}_i)}{\partial \xi_j} (\mathbf{L}^{\text{iso}} + \mathbf{L}^{\text{vol}}) \frac{\partial \mathbf{B}_L(\mathbf{A}_i)}{\partial \xi_j} + \frac{\partial \mathbf{B}_{NL}^T(\mathbf{A}_i)}{\partial \xi_j} (\mathbf{T}^{\text{iso}} + \mathbf{T}^{\text{vol}}) \frac{\partial \mathbf{B}_{NL}(\mathbf{A}_i)}{\partial \xi_j} \right)$$

and the isochoric stabilization term as

$$s_h^{\text{iso}} := \frac{J}{12} \sum_{j=1}^3 \left( \frac{\partial \mathbf{B}_L^T(\mathbf{A}_i)}{\partial \xi_j} \mathbf{L}^{\text{iso}} \frac{\partial \mathbf{B}_L(\mathbf{A}_i)}{\partial \xi_j} + \frac{\partial \mathbf{B}_{NL}^T(\mathbf{A}_i)}{\partial \xi_j} \mathbf{T}^{\text{iso}} \frac{\partial \mathbf{B}_{NL}(\mathbf{A}_i)}{\partial \xi_j} \right)$$

and thus we define “1-PStab” to mean

$$\mathbf{K}_T \approx J \left( \mathbf{B}_L^T (\mathbf{L}^{\text{iso}} + \mathbf{L}^{\text{vol}}) \mathbf{B}_L + \mathbf{B}_{NL}^T (\mathbf{L}^{\text{iso}} + \mathbf{L}^{\text{vol}}) \mathbf{B}_{NL} \right) + s_h$$

and

$$\mathbf{g} = \int_T \mathbf{B}_L^T \mathbf{S} dx_1 dx_2 dx_3 \approx J \mathbf{B}_L^T (\mathbf{S}^{\text{iso}} + \mathbf{S}^{\text{vol}}) + s_h.$$

Furthermore we define “1-PStabIso” to mean

$$\mathbf{K}_T \approx J \left( \mathbf{B}_L^T (\mathbf{L}^{\text{iso}} + \mathbf{L}^{\text{vol}}) \mathbf{B}_L + \mathbf{B}_{NL}^T (\mathbf{L}^{\text{iso}} + \mathbf{L}^{\text{vol}}) \mathbf{B}_{NL} \right) + s_h^{\text{iso}}$$

and

$$\mathbf{g} = \int_T \mathbf{B}_L^T \mathbf{S} dx_1 dx_2 dx_3 \approx J \mathbf{B}_L^T (\mathbf{S}^{\text{iso}} + \mathbf{S}^{\text{vol}}) + s_h^{\text{iso}}.$$

Lastly, we consider the case when the stabilization term is defined using  $\mathbf{A}_i = \mathbf{0}$ , i.e., using a constant approximation for the Jacobian. We define “1-PStabConstJ” to mean  $s_h|_{\mathbf{A}_i=\mathbf{0}}$  and “1-PStabIsoConstJ” to mean  $s_h^{\text{iso}}|_{\mathbf{A}_i=\mathbf{0}}$ .

### 4.3 Cantilever beam

We consider the case of a cantilever with dimensions

$$0 \leq x_1 \leq 1/2, \quad 0 \leq x_2 \leq 1/10, \quad 0 \leq x_3 \leq 1/10,$$

in meters and with zero displacements at  $x = 0$ . This Cantilever was subjected to an external virtual work

$$l(\mathbf{v}) = \int_{\Omega_0} \mathbf{f} \cdot \mathbf{v} d\Omega$$

with  $\mathbf{f} = (0, 0, -10)\text{GN/m}^3$ . The moduli of elasticity were chosen as  $E = 200\text{GPa}$ ,  $\nu = 0.33$ . For the Mooney-Rivlin model, we chose to define the bulk moduls as  $K = E/(3(1-\nu))$ ,  $K_1 = E/(2(1+\nu))$  and  $K_2 = 0$  effectively reducing the model to a Neo-Hookean material model.

We compare the one point integration rule with stabilization, which converges rapidly to the solution in Figure 1b, to the result obtained using full integration in Figure 1a which shows that the difference in maximum tip displacement is small for this particular meshsize.

### 4.4 Stiffness comparison

We compare the tip deflection of the cantilever computed using different integration schemes for a fixed load with decreasing meshsizes. We compare the one-point integration with stabilization to full integration and the classical reduced integration. Using the same parameters as in the previous section we measure the tip displacement using different meshsizes. We start with a uniform mesh with  $2 \times 2 \times 10$  elements and use uniform refinement for each new mesh size. We show the obtained results in Figure 2, where it can be noticed that the one point integration with stabilization behaves almost exactly like the full integration and that the one point integration with stabilized isochoric term gives nearly identical results as the classical approach of one point integration of the volumetric term. The lack of stabilization on the volumetric term makes the one point integration with stabilization considerably softer than using stabilization on both terms.

In Figure 3, we compare the tip displacement for the different integration approaches under linearly increasing volume load. The load is linearly increasing from  $\mathbf{f} = (0, 0, -1)\text{GN/m}^3$  to  $\mathbf{f} = (0, 0, -10)\text{GN/m}^3$  and it can be seen that the one point integration with

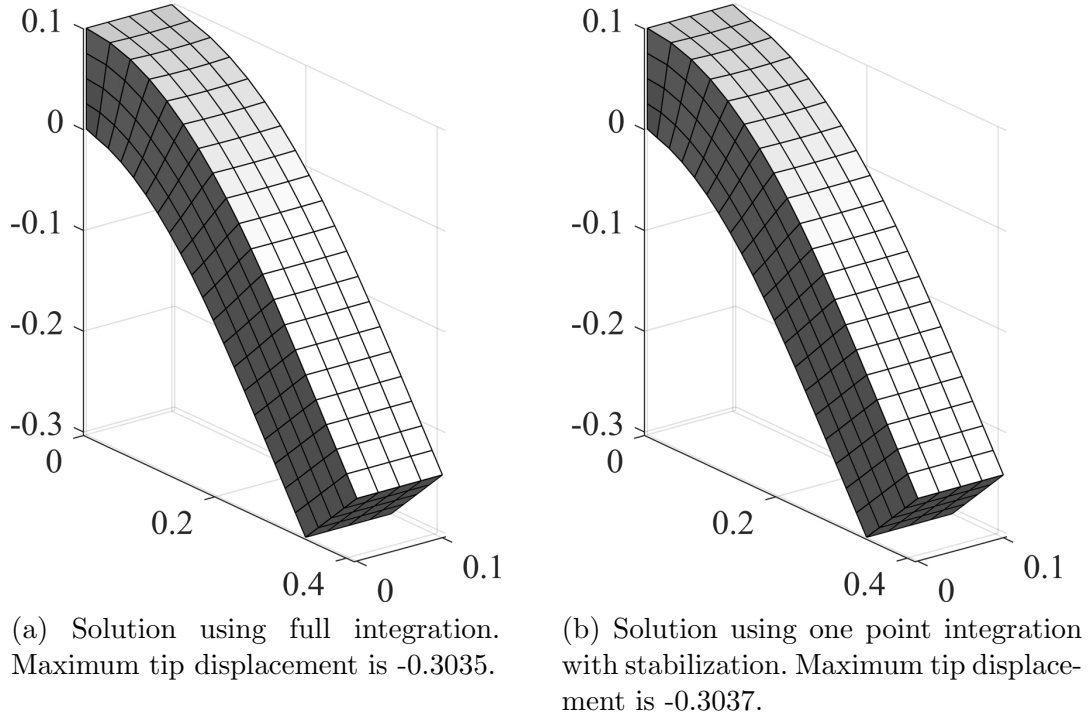


Fig. 1. Cantilever solution

stabilization approach continues to overlap with the full integration approach and that the same overlapping can be seen for the one point integration with stabilization of the isochoric term and the reduced integration.

#### 4.5 Near incompressibility

In Figure 4, we show the tip displacement of the same cantilever, load and material parameters from the previous Section as  $\nu \rightarrow 1/2$ . Notice the locking behavior when using full integration as well as one point integration with stabilization compared to one point integration of the volumetric term and one point integration with stabilization of the isochoric term. In our numerical test we were able to get stable solutions with  $\nu$  reaching up to  $\nu = 0.499$ .

#### 4.6 Mesh distortion

In order to investigate the sensitivity of the proposed one point integration schemes to mesh distortion we use a modified cantilever beam with a distortion parameter  $d$  as shown

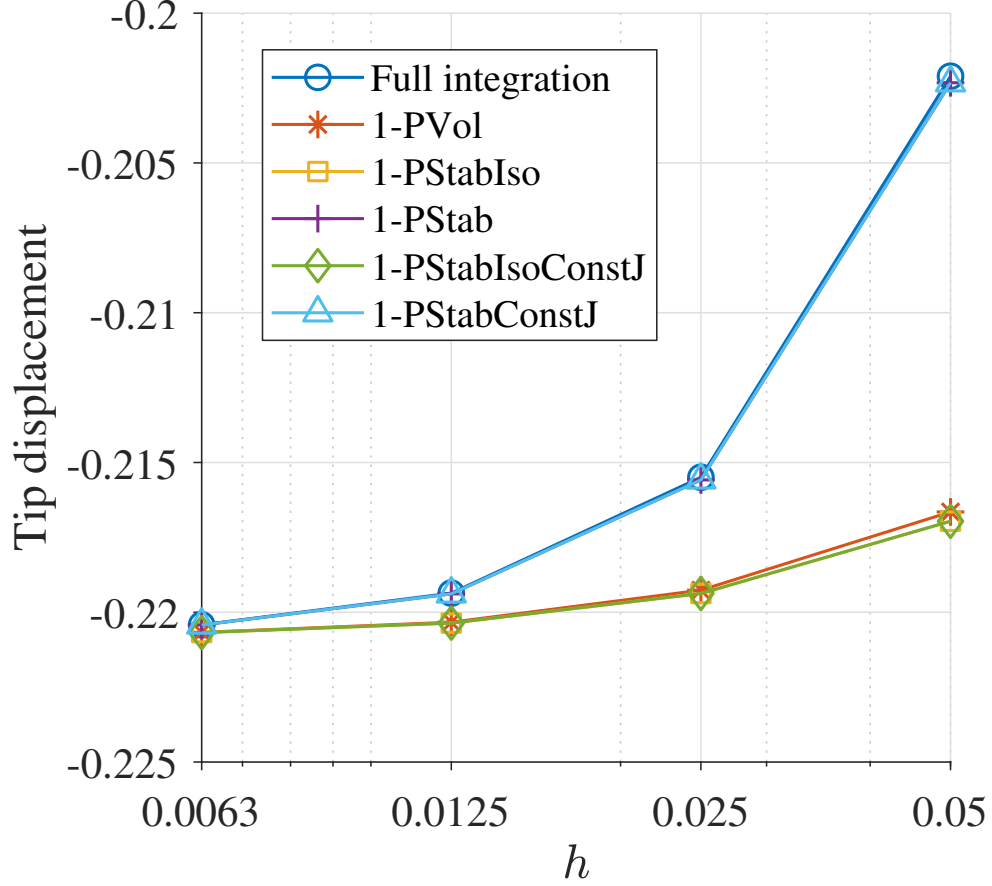


Fig. 2. Tip displacement under fixed load and uniformly changing meshsize using different integration methods.

in Figure 5a and the corresponding mesh is shown in Figure 5b. All other parameters of the model are the same as in the previous sections. We compared the relative change of the resultant of the tip displacement  $U_r$  with an increasing distortion parameter  $d$  from an initial distortion of  $d = 0$  to  $d = 0.2$ , so that  $U_r = U_r(d)$ . The results are presented in Figure 6, where the relative tip displacement is defined as

$$U_r^{\text{rel}} = 1 - U_r(d)/U_r(0).$$

Notice how the one point integration schemes diverge from the reference tip displacement with almost 60 to above 70% as the distortion becomes severe while the full integration and the classical reduced integration scheme remain relatively unaffected. This sensitivity to mesh distortion is compatible with the results of Reese et al. [7].

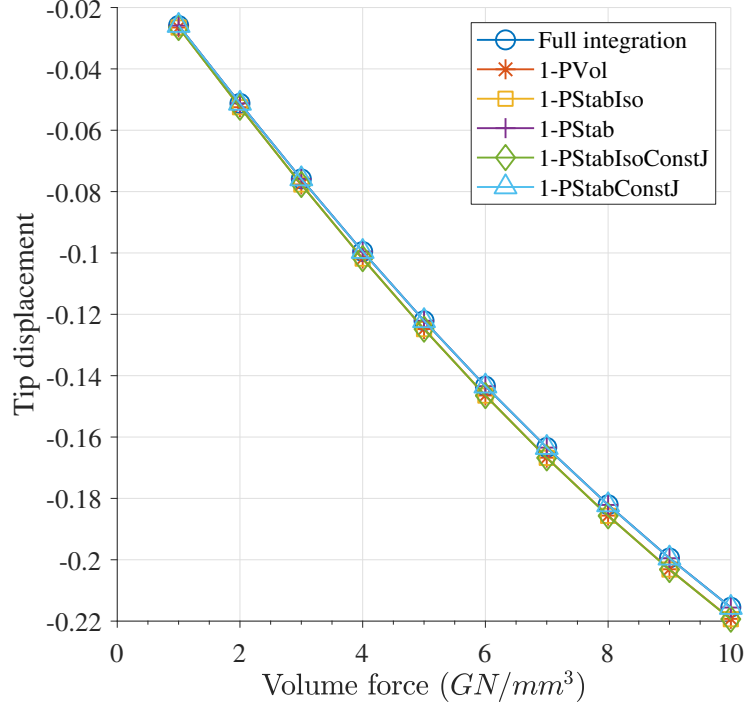


Fig. 3. Tip displacement under varying load using different integration methods.

#### 4.7 Linear elastic mesh distortion

We compare the sensitivity of the non-linear solution due to mesh distortion from Section 4.6 to a linear solution with the volumetric load  $\mathbf{f} = (0, 0, -1)$  GN/m<sup>3</sup>. The same beam geometry is used as in the previous section with the same distortion and material parameters on the same mesh. The results can be seen in Figure 7, where a clear similarity can be seen to the non-linear case, the one-point integration scheme does not integrate the determinant of the Jacobian accurately enough.

## 5 Concluding remarks

We have presented a general approach for one point integration of bi- and tri-linear finite elements in large deformation elasticity. The approach is related to Taylor expansion ideas [4,7] but with a focus on integration.

The basic method is highly accurate on meshes that do not contain highly distorted elements but shows an artificial stiffening as the element distortion increases, which is in

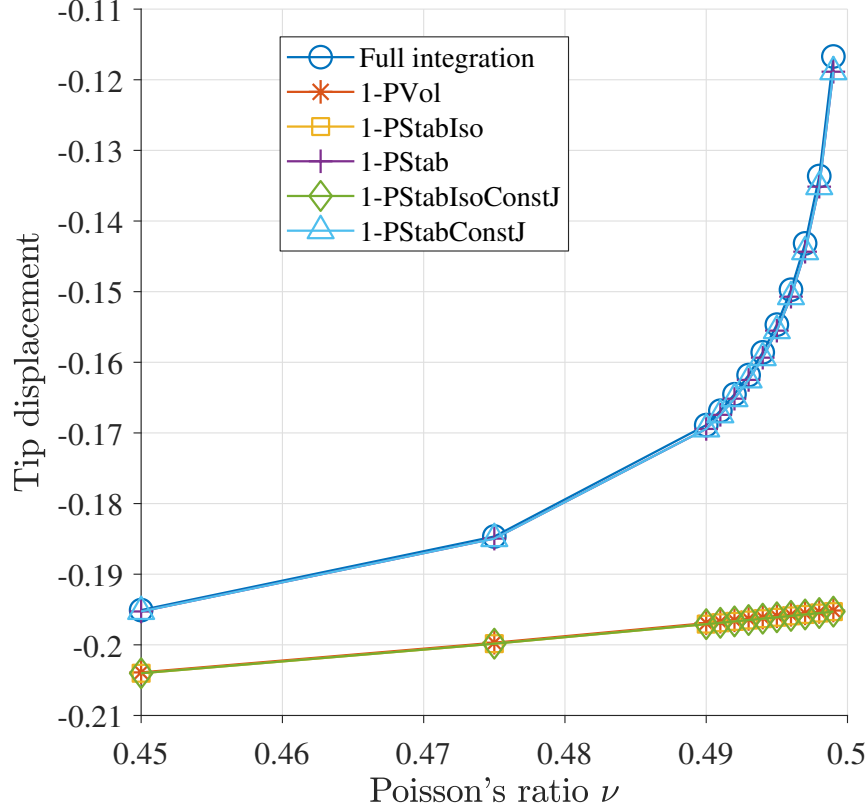


Fig. 4. Locking behavior with Full integration / one point integration with stabilization versus the locking free solution using reduced integration / one point integration of the isochoric term.

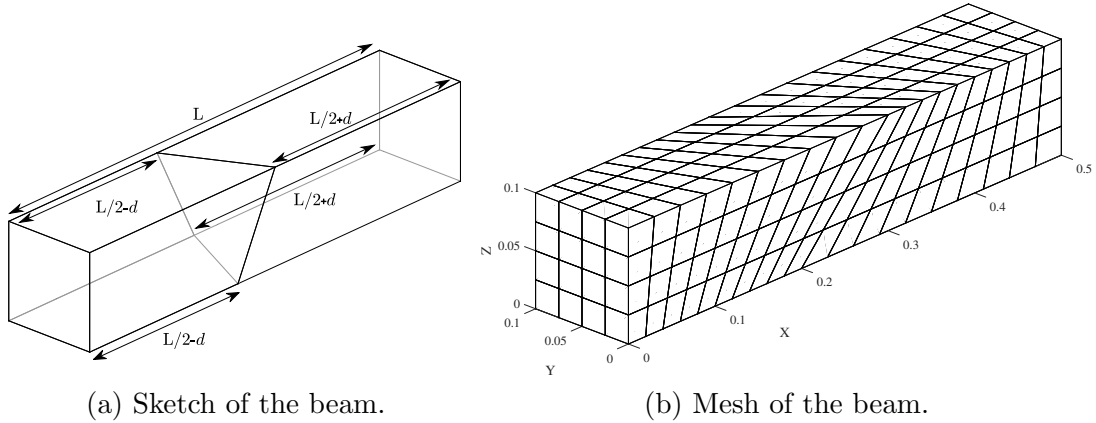


Fig. 5. Beam used to investigate sensitivity to mesh distortion

accord with other hourglass stabilization methods. We therefore proposed a further modification which takes into account the effect of element distortion more accurately. This rule shows results close to the standard  $2 \times 2 \times 2$  Gauss rule also on severely distorted meshes.



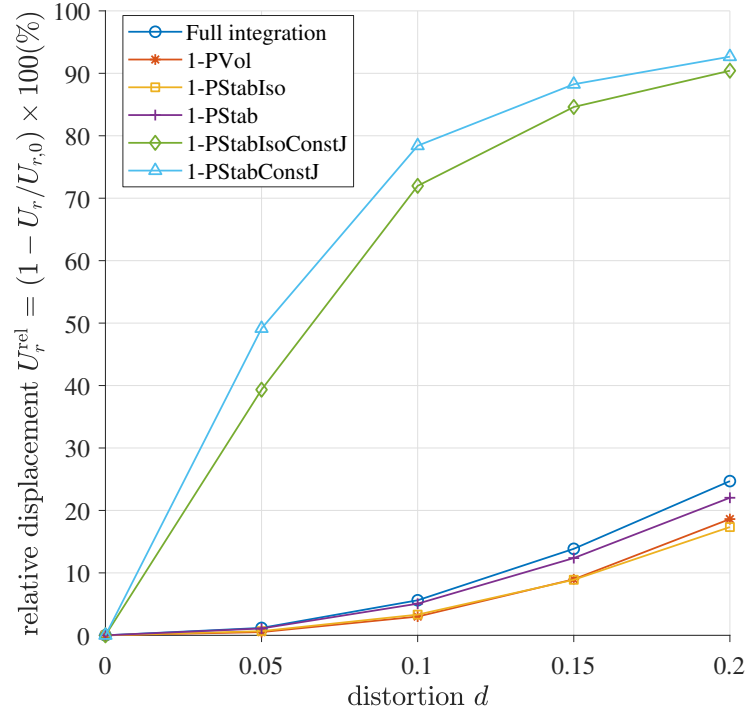


Fig. 6. Effects of mesh distortion on the relative tip displacement for the non-linear problem.

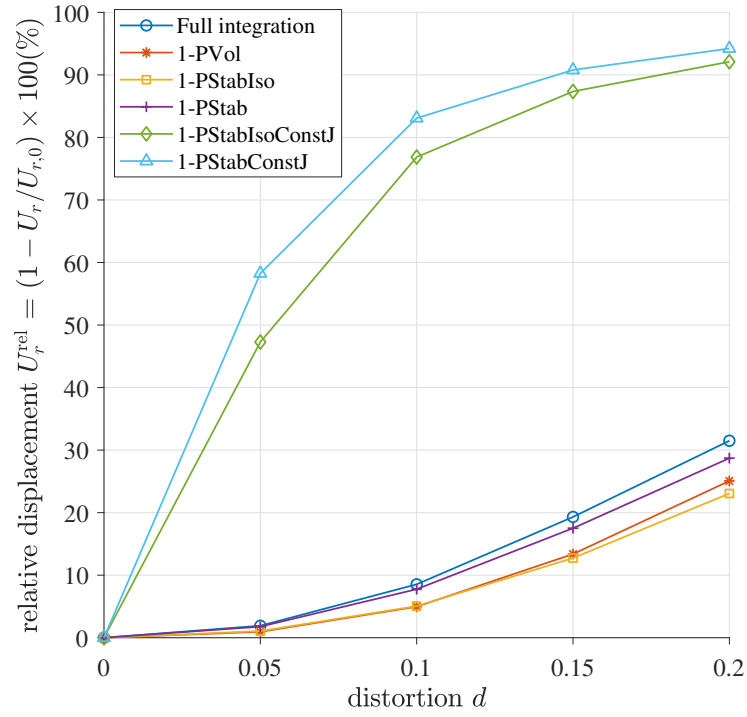


Fig. 7. Effects of mesh distortion on the relative tip displacement for the linear problem.

## Appendix

The linearisation is implemented using the Voigt form and the details are given below. We follow the notation of de Borst et al. [10] (which however contains misprints regarding the expressions for  $\frac{\partial I_2}{\partial \mathbf{C}}$  and  $\frac{\partial^2 I_3}{\partial \mathbf{C}^2}$ ).

In Voigt notation, the deformation gradient is computed by

$$\mathbf{F} = \begin{pmatrix} 1 & 0 & 0 & 0 & 1 & 0 & 0 & 0 & 1 \end{pmatrix}^T + \text{grad}\mathbf{U},$$

where  $\text{grad}\mathbf{U} = \mathbf{B}\mathbf{a}$  and

$$\mathbf{B} = \begin{bmatrix} \frac{\partial \varphi_1}{\partial x_1} & 0 & 0 & \frac{\partial \varphi_2}{\partial x_1} & 0 & 0 & \dots \\ \frac{\partial \varphi_1}{\partial x_2} & 0 & 0 & \frac{\partial \varphi_2}{\partial x_2} & 0 & 0 & \dots \\ \frac{\partial \varphi_1}{\partial x_3} & 0 & 0 & \frac{\partial \varphi_2}{\partial x_3} & 0 & 0 & \dots \\ 0 & \frac{\partial \varphi_1}{\partial x_1} & 0 & 0 & \frac{\partial \varphi_2}{\partial x_1} & 0 & \dots \\ 0 & \frac{\partial \varphi_1}{\partial x_2} & 0 & 0 & \frac{\partial \varphi_2}{\partial x_2} & 0 & \dots \\ 0 & \frac{\partial \varphi_1}{\partial x_3} & 0 & 0 & \frac{\partial \varphi_2}{\partial x_3} & 0 & \dots \\ 0 & 0 & \frac{\partial \varphi_1}{\partial x_1} & 0 & 0 & \frac{\partial \varphi_2}{\partial x_1} & \dots \\ 0 & 0 & \frac{\partial \varphi_1}{\partial x_2} & 0 & 0 & \frac{\partial \varphi_2}{\partial x_2} & \dots \\ 0 & 0 & \frac{\partial \varphi_1}{\partial x_3} & 0 & 0 & \frac{\partial \varphi_2}{\partial x_3} & \dots \end{bmatrix}.$$

The right Cauchy-Green tensor is then given by  $\mathbf{C} = \mathbf{F}^T \mathbf{F}$ . The derivatives of the invariants with respect to  $\mathbf{C}$  are given by

$$\frac{\partial I_1}{\partial \mathbf{C}} = \begin{pmatrix} 1 \\ 1 \\ 1 \\ 0 \\ 0 \\ 0 \end{pmatrix}, \quad \frac{\partial I_2}{\partial \mathbf{C}} = \begin{pmatrix} C_{33} + C_{22} \\ C_{11} + C_{33} \\ C_{22} + C_{11} \\ -C_{12} \\ -C_{23} \\ -C_{13} \end{pmatrix}, \quad \frac{\partial I_3}{\partial \mathbf{C}} = \begin{pmatrix} C_{22}C_{33} - C_{23}^2 \\ C_{33}C_{11} - C_{31}^2 \\ C_{11}C_{22} - C_{12}^2 \\ C_{23}C_{31} - C_{33}C_{12} \\ C_{31}C_{12} - C_{11}C_{23} \\ C_{12}C_{23} - C_{22}C_{31} \end{pmatrix}.$$

The derivatives of the modified invariants are given by

$$\begin{cases} \frac{\partial J_1}{\partial \mathbf{C}} &= I_3^{-1/3} \frac{\partial I_1}{\partial \mathbf{C}} - \frac{1}{3} I_1 I_3^{-4/3} \frac{\partial I_3}{\partial \mathbf{C}} \\ \frac{\partial J_2}{\partial \mathbf{C}} &= I_3^{-2/3} \frac{\partial I_2}{\partial \mathbf{C}} - \frac{2}{3} I_2 I_3^{-5/3} \frac{\partial I_3}{\partial \mathbf{C}} \\ \frac{\partial J_3}{\partial \mathbf{C}} &= \frac{1}{2} I_3^{-1/2} \frac{\partial I_3}{\partial \mathbf{C}} \end{cases}$$

The second derivatives of the invariants are given by

$$\frac{\partial^2 I_1}{\partial \mathbf{C}^2} = \mathbf{0},$$

$$\frac{\partial^2 I_2}{\partial \mathbf{C}^2} = \begin{bmatrix} 0 & 1 & 1 & 0 & 0 & 0 \\ 1 & 0 & 1 & 0 & 0 & 0 \\ 1 & 1 & 0 & 0 & 0 & 0 \\ 0 & 0 & 0 & -1/2 & 0 & 0 \\ 0 & 0 & 0 & 0 & -1/2 & 0 \\ 0 & 0 & 0 & 0 & 0 & -1/2 \end{bmatrix},$$

and

$$\frac{\partial^2 I_3}{\partial \mathbf{C}^2} = \begin{bmatrix} 0 & C_{33} & C_{22} & 0 & -C_{23} & 0 \\ C_{33} & 0 & C_{11} & 0 & 0 & -C_{31} \\ C_{22} & C_{11} & 0 & -C_{12} & 0 & 0 \\ 0 & 0 & -C_{12} & -C_{33}/2 & C_{31}/2 & C_{23}/2 \\ -C_{23} & 0 & 0 & C_{31}/2 & -C_{11}/2 & C_{12}/2 \\ 0 & -C_{31} & 0 & -C_{23}/2 & C_{12}/2 & -C_{22}/2 \end{bmatrix}.$$

The second derivatives of the modified invariants are then given by

$$\left\{ \begin{array}{l} \frac{\partial^2 J_1}{\partial \mathbf{C}^2} = I_3^{-1/3} \frac{\partial^2 I_1}{\partial \mathbf{C}^2} + \frac{4}{9} I_1 I_3^{-7/3} \frac{\partial I_3}{\partial \mathbf{C}} \left( \frac{\partial I_3}{\partial \mathbf{C}} \right)^T \\ \quad - \frac{1}{3} I_3^{-4/3} \left[ \frac{\partial I_1}{\partial \mathbf{C}} \left( \frac{\partial I_1}{\partial \mathbf{C}} \right)^T + I_1 \frac{\partial^2 I_3}{\partial \mathbf{C}^2} + \frac{\partial I_3}{\partial \mathbf{C}} \left( \frac{\partial I_3}{\partial \mathbf{C}} \right)^T \right] \\ \frac{\partial^2 J_2}{\partial \mathbf{C}^2} = I_3^{-2/3} \frac{\partial^2 I_2}{\partial \mathbf{C}^2} + \frac{10}{9} I_2 I_3^{-8/3} \frac{\partial I_3}{\partial \mathbf{C}} \left( \frac{\partial I_3}{\partial \mathbf{C}} \right)^T \\ \quad - \frac{2}{3} I_3^{-5/3} \left[ \frac{\partial I_2}{\partial \mathbf{C}} \left( \frac{\partial I_3}{\partial \mathbf{C}} \right)^T + I_2 \frac{\partial^2 I_3}{\partial \mathbf{C}^2} + \frac{\partial I_3}{\partial \mathbf{C}} \left( \frac{\partial I_2}{\partial \mathbf{C}} \right)^T \right] \\ \frac{\partial^2 J_3}{\partial \mathbf{C}^2} = \frac{1}{2} I_3^{-1/2} \frac{\partial^2 I_3}{\partial \mathbf{C}^2} - \frac{1}{4} I_3^{-3/2} \frac{\partial I_3}{\partial \mathbf{C}} \left( \frac{\partial I_3}{\partial \mathbf{C}} \right)^T \end{array} \right. .$$

The second Piola-Kirchhoff tensor on Voigt form is given as:

$$\left\{ \begin{array}{l} \mathbf{S}_{\text{iso}} = 2 \left( K_1 \frac{\partial J_1}{\partial \mathbf{C}} + K_2 \frac{\partial J_2}{\partial \mathbf{C}} \right) \\ \mathbf{S}_{\text{vol}} = 2K (J_3 - 1) \frac{\partial J_3}{\partial \mathbf{C}} \end{array} \right.$$

where  $J_3 = I_3^{\frac{1}{2}}$ . The constitutive forth order tensor is given on Voigt form as:

$$\left\{ \begin{array}{l} \mathbf{L}_{\text{iso}} = 4 \left( K_1 \frac{\partial^2 J_1}{\partial \mathbf{C}^2} + K_2 \frac{\partial^2 J_2}{\partial \mathbf{C}^2} \right) \\ \mathbf{L}_{\text{vol}} = 4 \left( K (J_3 - 1) \frac{\partial^2 J_3}{\partial \mathbf{C}^2} + K \frac{\partial J_3}{\partial \mathbf{C}} \otimes \frac{\partial J_3}{\partial \mathbf{C}} \right) \end{array} \right. .$$

The B-matrices used in the previous sections are given as follows:

$$\mathbf{B}_L = \begin{bmatrix} F_{11} \frac{\partial \varphi^1}{\partial x} & F_{21} \frac{\partial \varphi^1}{\partial x} & F_{31} \frac{\partial \varphi^1}{\partial x} & \dots \dots \\ F_{12} \frac{\partial \varphi^1}{\partial y} & F_{22} \frac{\partial \varphi^1}{\partial y} & F_{32} \frac{\partial \varphi^1}{\partial y} & \dots \dots \\ F_{13} \frac{\partial \varphi^1}{\partial z} & F_{23} \frac{\partial \varphi^1}{\partial z} & F_{33} \frac{\partial \varphi^1}{\partial z} & \dots \dots \\ F_{11} \frac{\partial \varphi^1}{\partial y} + F_{12} \frac{\partial \varphi^1}{\partial x} & F_{21} \frac{\partial \varphi^1}{\partial y} + F_{22} \frac{\partial \varphi^1}{\partial x} & F_{31} \frac{\partial \varphi^1}{\partial y} + F_{32} \frac{\partial \varphi^1}{\partial x} & \dots \dots \\ F_{12} \frac{\partial \varphi^1}{\partial z} + F_{13} \frac{\partial \varphi^1}{\partial y} & F_{22} \frac{\partial \varphi^1}{\partial z} + F_{23} \frac{\partial \varphi^1}{\partial y} & F_{32} \frac{\partial \varphi^1}{\partial z} + F_{33} \frac{\partial \varphi^1}{\partial y} & \dots \dots \\ F_{13} \frac{\partial \varphi^1}{\partial x} + F_{11} \frac{\partial \varphi^1}{\partial z} & F_{23} \frac{\partial \varphi^1}{\partial x} + F_{21} \frac{\partial \varphi^1}{\partial z} & F_{33} \frac{\partial \varphi^1}{\partial x} + F_{31} \frac{\partial \varphi^1}{\partial z} & \dots \dots \end{bmatrix},$$

$$\mathbf{B}_{NL} = \begin{bmatrix} \frac{\partial \varphi^1}{\partial x} & 0 & 0 & \dots \dots \\ \frac{\partial \varphi^1}{\partial y} & 0 & 0 & \dots \dots \\ \frac{\partial \varphi^1}{\partial z} & 0 & 0 & \dots \dots \\ 0 & \frac{\partial \varphi^1}{\partial x} & 0 & \dots \dots \\ 0 & \frac{\partial \varphi^1}{\partial y} & 0 & \dots \dots \\ 0 & \frac{\partial \varphi^1}{\partial z} & 0 & \dots \dots \\ 0 & 0 & \frac{\partial \varphi^1}{\partial x} & \dots \dots \\ 0 & 0 & \frac{\partial \varphi^1}{\partial y} & \dots \dots \\ 0 & 0 & \frac{\partial \varphi^1}{\partial z} & \dots \dots \end{bmatrix},$$

and for the higher order terms in the stabilization we define the derivatives of the B-matrices as follows:

$$\frac{\partial \mathbf{B}_L}{\partial \xi_i} = \begin{bmatrix} F_{11} \varphi_x^1 & F_{21} \varphi_x^1 & F_{31} \varphi_x^1 & \dots \dots \\ F_{12} \varphi_y^1 & F_{22} \varphi_y^1 & F_{32} \varphi_y^1 & \dots \dots \\ F_{13} \varphi_z^1 & F_{23} \varphi_z^1 & F_{33} \varphi_z^1 & \dots \dots \\ F_{11} \varphi_y^1 + F_{12} \varphi_x^1 & F_{21} \varphi_y^1 + F_{22} \varphi_x^1 & F_{31} \varphi_y^1 + F_{32} \varphi_x^1 & \dots \dots \\ F_{12} \varphi_z^1 + F_{13} \varphi_y^1 & F_{22} \varphi_z^1 + F_{23} \varphi_y^1 & F_{32} \varphi_z^1 + F_{33} \varphi_y^1 & \dots \dots \\ F_{13} \varphi_x^1 + F_{11} \varphi_z^1 & F_{23} \varphi_x^1 + F_{21} \varphi_z^1 & F_{33} \varphi_x^1 + F_{31} \varphi_z^1 & \dots \dots \end{bmatrix},$$

where  $\varphi_x = \frac{\partial}{\partial \xi_i} \left( \frac{\partial \varphi}{\partial x} \right)$ . The derivatives of  $\mathbf{B}_{NL}$  are given as:

$$\frac{\partial \mathbf{B}_{NL}}{\partial \xi_i} = \begin{bmatrix} \varphi_x^1 & 0 & 0 & \varphi_x^2 & 0 & 0 & \dots \\ \varphi_y^1 & 0 & 0 & \varphi_y^2 & 0 & 0 & \dots \\ \varphi_z^1 & 0 & 0 & \varphi_z^2 & 0 & 0 & \dots \\ 0 & \varphi_x^1 & 0 & 0 & \varphi_x^2 & 0 & \dots \\ 0 & \varphi_y^1 & 0 & 0 & \varphi_y^2 & 0 & \dots \\ 0 & \varphi_z^1 & 0 & 0 & \varphi_z^2 & 0 & \dots \\ 0 & 0 & \varphi_x^1 & 0 & 0 & \varphi_x^2 & \dots \\ 0 & 0 & \varphi_y^1 & 0 & 0 & \varphi_y^2 & \dots \\ 0 & 0 & \varphi_z^1 & 0 & 0 & \varphi_z^2 & \dots \end{bmatrix},$$

where again  $\varphi_x = \frac{\partial}{\partial \xi_i} \left( \frac{\partial \varphi}{\partial x} \right)$ , etc. Note that on the tri-linear hexahedral element  $\frac{\partial}{\partial \xi_i} \left( \frac{\partial \varphi}{\partial x} \right)$  is constant for  $i=1, 2, 3$ .

## References

- [1] S. Glaser, F. Armero, On the formulation of enhanced strain finite elements in finite deformations, *Eng. Comput.* 14 (7) (1997) 759–791.
- [2] S. Reese, M. Küssner, B. D. Reddy, A new stabilization technique for finite elements in non-linear elasticity, *Internat. J. Numer. Methods Engrg.* 44 (11) (1999) 1617–1652.
- [3] S. Reese, P. Wriggers, A stabilization technique to avoid hourglassing in finite elasticity, *Internat. J. Numer. Methods Engrg.* 48 (1) (2000) 79–109.
- [4] J. C. Schulz, Finite element hourglassing control, *Internat. J. Numer. Methods Engrg.* 21 (6) (1985) 1039–1048.
- [5] W. K. Liu, J. S.-J. Ong, R. A. Uras, Finite element stabilization matrices—a unification approach, *Comput. Methods Appl. Mech. Engrg.* 53 (1) (1985) 13–46.
- [6] W. K. Liu, T. Belytschko, J. S. J. Ong, S. E. Law, Use of stabilization matrices in non-linear analysis, *Eng. Comput.* 2 (1) (1985) 47–55.
- [7] S. Reese, P. Wriggers, B. D. Reddy, A new locking-free brick element technique for large deformation problems in elasticity, *Comput. & Structures* 75 (3) (2000) 291–304.
- [8] P. Hansbo, A new approach to quadrature for finite elements incorporating hourglass control as a special case, *Comput. Methods Appl. Mech. Engrg.* 158 (3-4) (1998) 301–309.
- [9] P. Hansbo, F. Larsson, The nonconforming linear strain tetrahedron for a large deformation elasticity problem, *Comput. Mech.* 58 (6) (2016) 929–935.

- [10] R. de Borst, M. A. Crisfield, J. J. C. Remmers, C. V. Verhoosel, Nonlinear finite element analysis of solids and structures, 2nd Edition, John Wiley & Sons, 2012.